

Imprinting strategies for 100 nm lithography on polyfluorene and poly(phenylenevinylene) derivatives and their blends

Elisa Mele ^{*}, Andrea Camposeo, Pompilio Del Carro, Francesca Di Benedetto, Ripalta Stabile, Luana Persano, Roberto Cingolani, Dario Pisignano

NNL, National Nanotechnology Laboratory of CNR-INFN, Dipartimento di Ingegneria dell'Innovazione, Università degli Studi di Lecce, c/o Distretto Tecnologico ISUFI, via Arnesano, I-73100 Lecce, Italy

Received 7 May 2006; received in revised form 10 July 2006; accepted 10 July 2006
Available online 14 August 2006

Abstract

We report on the use of nanoimprint lithography at room temperature (RT-NIL) for the direct structuring of polyfluorene and poly(phenylenevinylene) derivatives and of their blends without the degradation of the emissive characteristics of the active molecules. We apply RT-NIL for the fabrication of periodic one- and two-dimensional gratings with feature width that varies from 100 to 500 nm. Moreover, we analysed the effects that a superimposed periodic corrugation induces on the emitted light in terms of spectral properties and luminescence efficiency, thus ruling out any degradation of the emission. In particular, the combination of nanopatterning and active blends opens new perspectives for the control of the emitted colour from conjugated polymer films.

© 2006 Elsevier B.V. All rights reserved.

Keywords: Nanoimprint lithography; Conjugated polymers; Nanophotonics; Photo crystals; Organic gratings

1. Introduction

The nanoimprint lithography (NIL) is a straightforward and high throughput technique for producing patterns onto a wide range of materials, both optically and electronically inert [1,2] and active organics [3,4], up to a resolution of sub-10 nm. In the NIL process, high resolution polymeric features are fabricated by the irreversible deformation of the surface morphology of a thermoplastic film under the simultaneous application of pressure and temperature. In particular, the pattern originally present on the surface of a rigid mold, previously realised by conventional approaches such as photo- or electron-beam lithography, is transferred into a film of a thermoplastic polymer coating a substrate. This is achieved by heating the polymeric layer above its glass transition temperature (T_g , generally up to 200 °C) and by applying external pressure (about 100 MPa). As a consequence of the high temperature, the polymer viscosity decreases dramatically, and the organic material fills the void spaces between the template and the film. Finally, the temperature is decreased below

T_g and the mold is mechanically removed. Thus, a negative copy of the starting pattern is transferred into the polymeric film. The mechanical operation principle of NIL allows one to overcome the resolution limitations related to the light diffraction, and its remarkable operational simplicity strongly reduces the overall costs of lithography.

Despite these advantages with respect to conventional lithographic methods that make the standard NIL ideal for patterning inert polymers and resists, this technology presents significant drawbacks for the direct structuring of organic light-emitting compounds in air. In fact, the cycle of high temperature required during the patterning step can determine a strong and irreversible degradation of the optical and electrical properties of the active employed materials, because of the occurrence of oxygen incorporation and substitution into the molecular backbones [5]. This important issue determines the necessity to carry out the imprinting onto conjugated molecules in a controlled atmosphere [4]. However, the use of vacuum or nitrogen chambers has as consequence the reduction of the NIL operation simplicity and the increment of the overall cost of the lithography.

Other patterning methods working at room temperature have been implemented for organic-based optoelectronic systems

^{*} Corresponding author. Tel.: +39 0832 298165; fax: +39 0832 298238.
E-mail address: elisa.mele@unile.it (E. Mele).

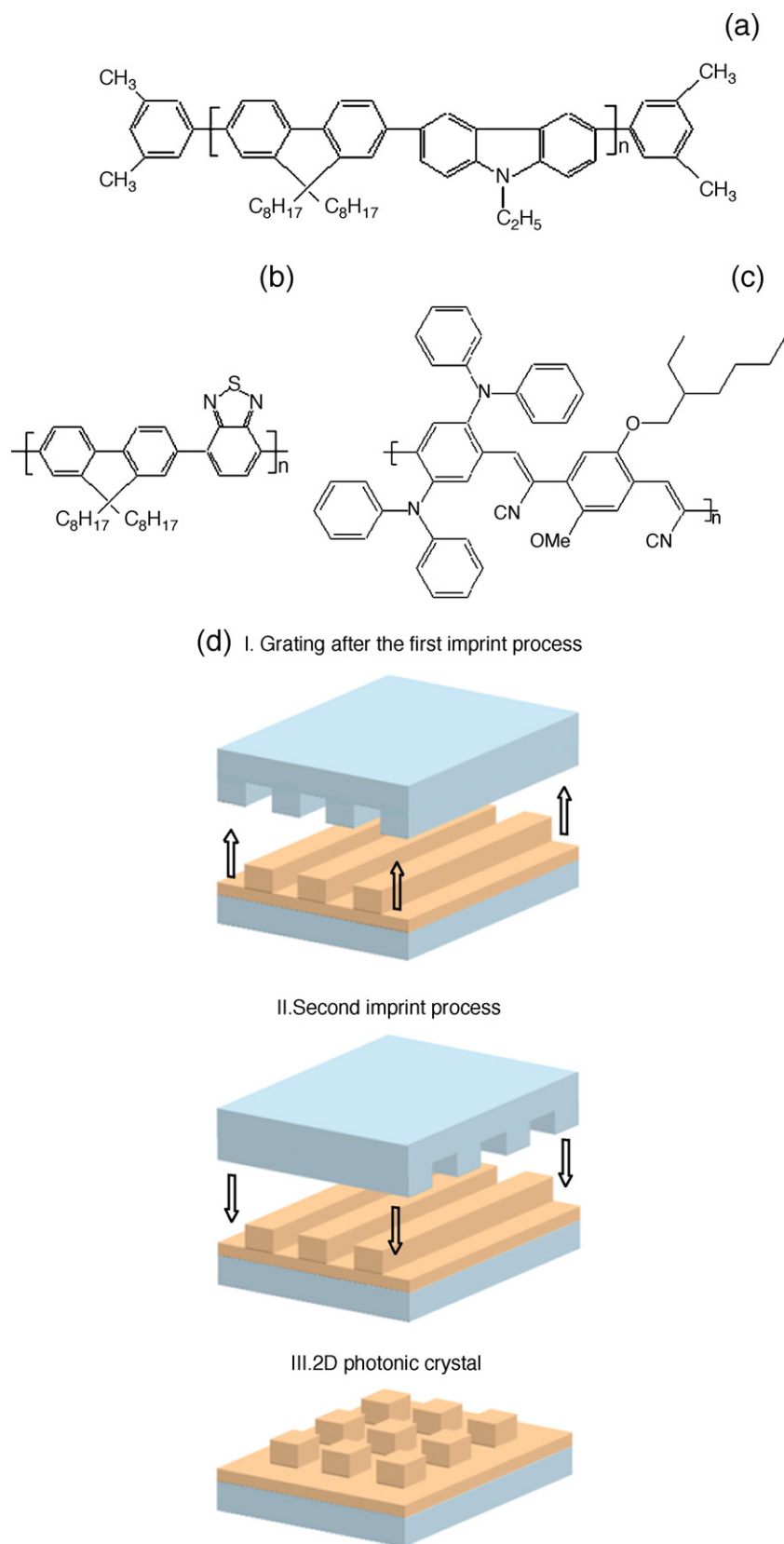


Fig. 1. Molecular structures of the employed polymers: (a) the blue-emitting polyfluorene derivative, (b) the yellow-emitting polyfluorene derivative and (c) the red emitter poly(phenylenevinylene) derivative. (d) Schematic diagram of the RT-NIL process for the realization of 1D and 2D PhC-like patterns (features not in scale).

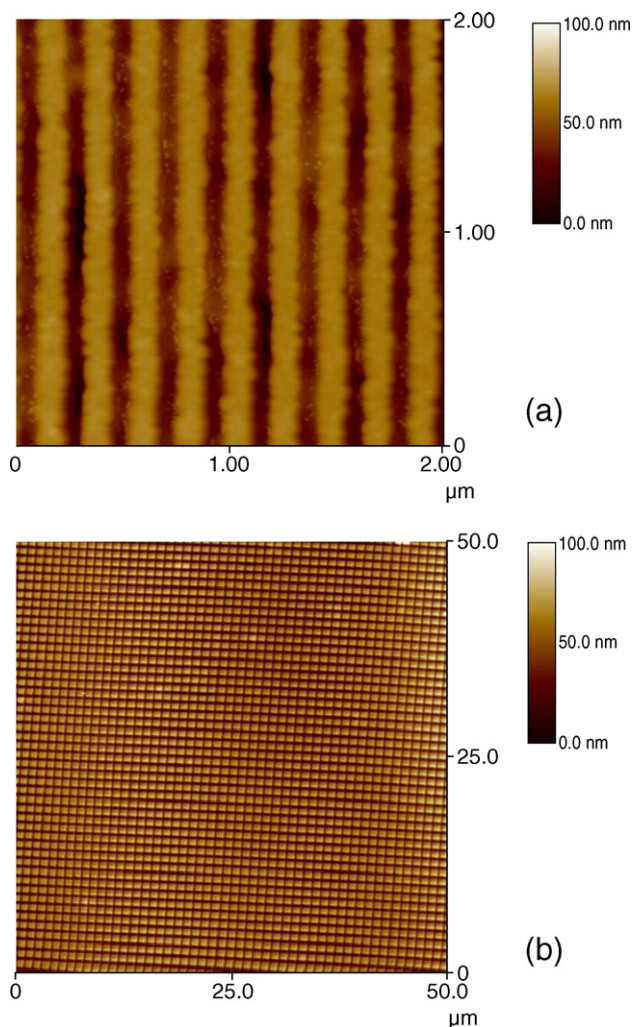


Fig. 2. AFM planar topographic views of patterns realized on the RE compound: (a) a 1D 200 nm period, grating ($2 \times 2 \mu\text{m}^2$), and (b) a 2D pattern with 500 nm feature size ($50 \times 50 \mu\text{m}^2$).

and microelectronic devices, such as field effect transistors [6] and light-emitting diode pixel arrays [7]. Such alternative technologies include soft lithographies [8] (namely microcontact printing (μCP) [9] and solvent-assisted micromolding [10]), screen printing [11], ink-jet printing [12] and step and flash lithography [13]. Imprinting-like approaches, such as μCP or step and flash methods, rely either on the use of elastomeric elements or on templated photopolymerisation. They are therefore very suitable for low-molar-mass molecular monolayers and for UV-curable polymers, respectively, whereas they are generally hardly compatible with conjugated polymers.

In previous studies, we wanted to apply the NIL technique for the fabrication of organic-based devices, and particularly organic lasers which have to be pumped by high excitation densities (in the range of $10^{-1} \mu\text{J cm}^{-2}$ – 10 mJ cm^{-2}) and which are therefore particularly demanding in terms of preserved functionality of the active molecules. For retaining the light-emitting performances of the molecules, we developed the NIL at room temperature (RT-NIL) on active organic materials, both non-thermoplastic oligomers [14] and conjugated polymers [15]. The RT-NIL has

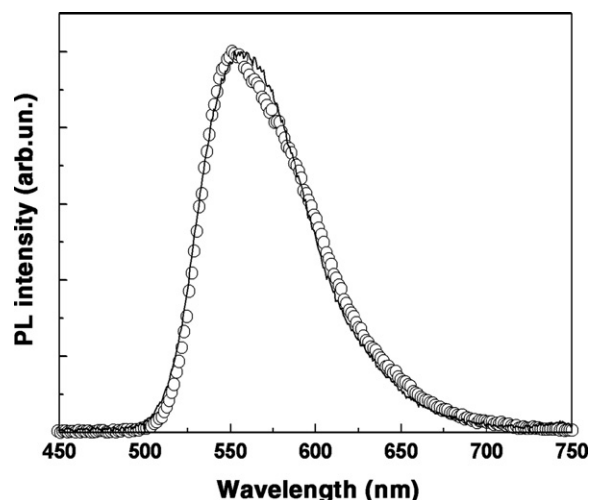


Fig. 3. Integrated PL spectra before (continuous line) and after (empty circles) the RT-NIL process for the YE film.

been initially proposed by Khang et al., as an alternative to conventional NIL for nanostructuring thermoplastic polymers, in order to reduce the difficulties met in hot embossing during the mold release and the distortions of the imprinted structures [16]. We observed that, by avoiding thermal cycles in the imprinting procedure, one can pattern active organic materials in air without degradation of the emission properties [14], realizing complex features, also with two-dimensional (2D) patterns by simply repeating sequentially the imprinting step on the same region of the target film. The repeated imprinting is not possible by conventional hot embossing [15].

Among the wide range of organic light-emitting materials, the fluorene-based polymers and the poly(phenylenevinylene) derivatives are particularly interesting prototype molecules, since they exhibit high optical gain and excellent luminescence properties in all the visible range. To date, they found applications in light-emitting diodes [17,18], lasers [19–21], light-emitting

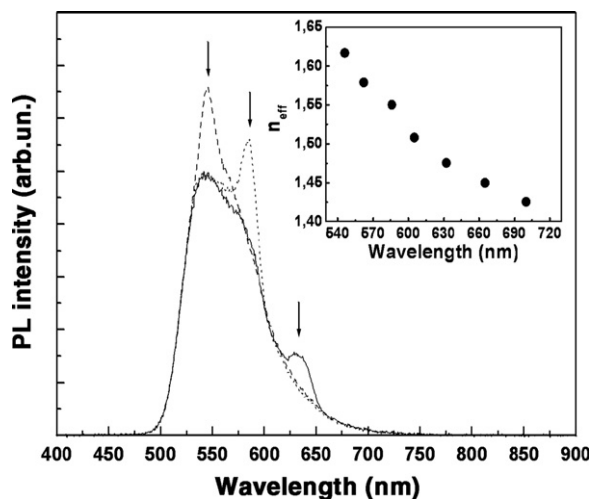


Fig. 4. PL spectra from the 1D imprinted grating (period 520 nm) at $\Theta=25^\circ$ (continuous line), 35° (dotted line) and 45° (dashed line) for the polyfluorene derivative. The arrows indicate the peak shift upon increasing the detection angle. Inset: wavelength dependence of n_{eff} .

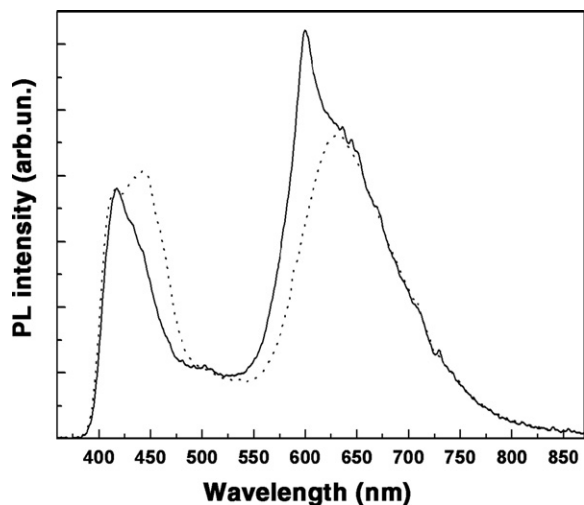


Fig. 5. PL spectra from the untextured sample (dotted line) and 1D imprinted grating (period 600 nm, $\theta=25^\circ$, continuous line) for a BE/RE blend.

electrochemical cells [22] and plastic solar cells [23,24]. Moreover, several reports described the possibility of engineering and controlling the light emission of conjugated compounds by the combination with optically active semiconductor nanocrystals [25], the realization of suitably calibrated blends [26,27] and the insertion of a 1D or 2D photonic crystal (PhC) structure [28]. Consequently, lithographic approaches able to realize wavelength-scale periodic nanostructures onto organic-based (monocomponent, blended or nanocomposite) emissive films, preserving their optoelectronic characteristics, are strongly required.

In this paper, we report our recent studies on the flexibility of RT-NIL for directly structuring organic light emitting polymeric films. With respect to previous experiments [15], we further extended the range of resolution achievable on conjugated polymers, obtaining 100 nm features, preserving at the same time the spectral characteristics and the luminescence efficiency of the molecules. In particular, we apply RT-NIL for fabricating periodic 1D and 2D features on polyfluorene and poly(phenylenevinylene) derivatives and their blends. Nanostructuring polymeric blends is particularly interesting since it allows one to effectively, fully control the colour of light emission from the films. In particular, we observe that the realization of 1D PhCs onto blend layers induces a blue-shift of the resulting emission upon observing the sample at an angle, $\theta=25^\circ$.

2. Experimental details

In our lithographic approach, we first realized master patterns with periodic parallel grooves having feature sizes of 100, 260, 300 and 500 nm onto silicon substrates. The masters were fabricated by a Raith 150 electron beam lithography system working at acceleration energy of 20 keV, and subsequent lift-off and reactive ion etching by CF_4/Ar . Then, the masters were directly exploited as templates for structuring films of polyfluorene and poly(phenylenevinylene) derivatives and their blends. The blue light-emitting polymer (BE, poly[(9,9-dihexylfluorenyl-2,7-diyl)-alt-co-(9,ethyl-3,6-carbazole)]), the yellow emitter (YE, poly[(9,9-dioctylfluorenyl-2,7-diyl)-co-(1,4-benzo-{2,1,3}-thia-

diazole)]) and the red emitter (RE, poly[{2-methoxy-5-(2-ethylhexyloxy)-1,4-(1-cyanovinylphenylene)-co-{2,5-bis(*N,N*-diphenylamino)-1,4-phenylene}]) were purchased from American Dye Source (Quebec, Canada) and used as received. The molecular structures of the BE, YE and RE compounds are displayed in Fig. 1a, b and c, respectively. Films of the YE polymer, of the RE one and of a BE:RE blend (1:500) were spin-coated at 2000 rpm for 40 s onto Corning glass substrates from a 1.3×10^{-4} M toluene solution, from a 1.5×10^{-3} M chloroform solution and from a 1.3×10^{-4} M dichloromethane solution, respectively.

The imprinting process was carried out by a two-column press (PW100 P/O/Weber, Germany) at room temperature, in air, with an applied force of about 1.5 kN [29]. The silicon template was manually positioned onto the active layer, and the system (stamp and substrate) was placed onto the lower plate of the press. The pressure onto the glass substrates (about $1 \times 1 \text{ cm}^2$ in size) supporting the thin films, applied by the lowering the higher plate of the press, was around 150 atm (15 MPa). No antisticking layer was needed in the imprinting process. Such patterning procedure was used for producing 1D gratings (period of 200, 520 and 600 nm) and 2D crossed patterns with 500 nm feature size by sequential multilevel imprinting. The scheme of the multilevel RT-NIL for the generation of 2D structures is shown in Fig. 1d. Once a 1D grating was realized onto the surface of the organic film, a second imprinting step was carried out onto the previously patterned area. The same rigid stamp was placed onto the first realized grating with an angle of 90° , namely by positioning the master silicon features perpendicular to the organic ones. When the mold was separated, a 2D pattern with 500 nm side squares was obtained on the polymeric film.

The photoluminescence (PL) spectra before and after the imprinting process were investigated by means of a fiber-coupled charge coupled device (CCD) (Ocean Optics) and by exciting the samples with a HeCd laser emitting at 325 nm. Angle-resolved PL measurements were carried out by collecting the light emitted in a small solid angle ($\approx 10^{-3}$ rad) around each value of angle, calculated by moving perpendicularly to the surface grating. The absolute quantum PL efficiency, η_{PL} , was measured by pumping the samples by a Xe lamp matched with a monochromator at an excitation wavelength of 390 nm. The number of PL photons per absorbed photon emitted by the film was determined by accounting for those photons which are not absorbed by the sample at their first incidence and are absorbed after successive reflections on the surface of the integrating sphere [30]:

$$\Phi_{\text{PL}} = \frac{P_1 - (1-\alpha)^2(R+T)P_2}{(1-R-T)(1-\alpha)X_L} \quad (1)$$

where R and T indicate the reflectance and transmittance of the system, respectively. In the previous expression, P_1 and P_2 are the photoluminescence signals measured with the lamp beam incident on the sample and on the integrating sphere, respectively, X_L stands for the excitation signal, measured with the beam incident on the sphere without the sample, and the factor $(1-\alpha)^2$ takes into account the correction due to the absorption of the glass substrate. All the signals were normalized by the spectral response of the experimental set-up.

3. Results and discussion

Light-emitting conjugated compounds are attractive materials for the realization of opto-electronic devices [18], because of their high luminescence quantum yield and optical gain. Consequently, many efforts have been done to develop simple and low cost techniques with optimal characteristics for applications in organic-based nanopatterned photonics, particularly for distributed feedback (DFB) lasers and photonic crystals (PhCs). For operation in the visible emission range, patterns have to be fabricated with feature size between 100 nm and 1 μm . The RT-NIL is a remarkably convenient method to fabricate organic structures of excellent quality in this range of resolutions. For instance, in Fig. 2a, we show the atomic force microscope (AFM) topographic image of a 200 nm periodic grating imprinted onto a layer of the RE polymer. The realized 1D pattern, exhibiting well-defined organic features, clearly suggests that the resolution achievable on conjugated polymers by RT-NIL can be even further increased, being strongly dependent on the starting master.

Moreover, a main advantage offered by RT-NIL with respect to hot embossing is the possibility to realize more complex 2D patterns by multiple imprinting steps on the same film with the same template. In conventional (high temperature) NIL, the heating of the thermoplastic layer required for the pattern transfer would destroy the previously embossed features; on the contrary, in RT-NIL, only the external pressure acts in order to deform the target film and to induce the wanted surface corrugation. The high pressure allows the polymer to reach its terminal flow region, where the time-dependent shear compliance, $J(t)$, exhibits a linear dependence on time, and the deformation becomes irreversible, and it also determines a contraction of the free volume available to molecules within the films, which on its turn causes an improved stability of the imprinted samples upon storage. In Fig. 2b, we display the AFM picture of a 2D imprinted organic grating with feature size of 500 nm.

In order to assess the possible influence of RT-NIL on the optical properties of the used light-emitting polymers, we measured their PL spectra before and after the imprinting process. In Fig. 3, the integrated PL spectrum of the YE compound is displayed. The spectrum does not present variations in the full width at half maximum (FWHM) and in the emission peak wavelength, λ_{PL} . We observed a FWHM value of 72 nm and $\lambda_{\text{PL}} = 553$ nm for the polyfluorene derivative. Analogously, the RE poly(phenylenevinylene) derivative shows $\lambda_{\text{PL}} = 646$ nm and FWHM = 90 nm, regardless of the RT-NIL. Thus, we conclude that the used patterning method fully preserves the integrated emission spectral properties of the active materials. In addition, we found that η_{PL} exhibits a value of 80% and 37% for the YE polymer and for the RE one, respectively, and no reduction in the PL efficiency was observed after carrying out the NIL procedure.

For the YE 1D grating with period 520 nm, we also analysed the effects of the superimposed periodic nanostructure on the luminescence properties by measuring the PL emission at different angles, Θ . The spectra of the imprinted YE film at 25°, 35° and 45° are shown in Fig. 4. The forward emission peak of

the printed distributed feedback structure is clearly visible, shifting from 700 nm (at 15°) to 546 nm (at 45°) with a strongly enhanced peak at 546 nm. The insertion of a 1D, wavelength-scale periodic grating onto the conjugated film allows the light trapped in waveguided modes within the organic slab to be scattered out of the film along certain forward directions [31,32]. Such enhanced Bragg-scattering of light reduces the effective length covered by the photons and, consequently, the self-absorption inside the organic layer, which can also result in an increase of the external quantum efficiency from the active slab. The dependence of the PL peak on the collection angle allows us to estimate the dependence of effective refractive index on wavelength, decreasing from 1.62 to 1.43 upon increasing λ from 546 to 700 nm (inset of Fig. 4).

Angle-resolved PL measurements were carried out also for a 1D grating (period 600 nm) imprinted onto the film of the BE/RE blend. In Fig. 5, the PL spectra for the untextured sample and the patterned one ($\Theta = 25^\circ$) are displayed. The modification of the spectral properties of the realized blends, induced by the insertion of the periodic corrugation, is demonstrated by the observed blue shift in the emission. This effect was evaluated by calculating the colour coordinates of the emitted light according to the Commission Internationale de l'Eclairage (CIE), which are given by the normalised projection of the emission spectrum, $S(\lambda)$, onto three colour matching functions, $\bar{x}(\lambda)$, $\bar{y}(\lambda)$ and $\bar{z}(\lambda)$, and are related to the perception response of the human eye:

$$X = \frac{\int_0^{+\infty} S(\lambda) \bar{x}(\lambda) d\lambda}{\sum}, \quad Y = \frac{\int_0^{+\infty} S(\lambda) \bar{y}(\lambda) d\lambda}{\sum} \quad \text{and} \quad Z = \frac{\int_0^{+\infty} S(\lambda) \bar{z}(\lambda) d\lambda}{\sum},$$

where $\sum = \sum_{\bar{x}, \bar{y}, \bar{z}} \int_0^{+\infty} S(\lambda) \bar{t}(\lambda) d\lambda$ (i.e. $X+Y+Z=1$). The colour can be therefore represented by its CIE coordinates in the bidimensional space (X, Y). In particular, the CIE coordinates are ($X=0.39, Y=0.23$) and ($X=0.46, Y=0.29$) for the untextured and for the structured blend films, respectively. The angle-resolved PL measurement of the grating reveals a 25% variation of the CIE coordinates (both for the X for Y), when the detection angle moves from 0° to 50°. Thus, the presence of a 1D grating offers the possibility to effectively tune the colour of the light emission achievable from polymeric blends. Further studies are currently in progress in our laboratory to properly design the geometry of the imprinted nanostructures in order to carefully enhance the emission of a desired spectral component, thus making possible to reach white emission ($X=0.39, Y=0.23$).

4. Conclusion

In conclusion, we demonstrated that RT-NIL is a suitable method for realizing high resolution structures onto polyfluorene and poly(phenylenevinylene) derivatives layers, and we further extend the resolution achievable on conjugated polymers to 100 nm. In particular, we produced both 1D and 2D light-emitting periodic gratings, and we could assess that the RT-NIL does not cause degradation of the emission properties of the employed materials. The combination of nanopatterning and active blends opens new perspectives for the control of the emitted colour from conjugated polymer films.

Acknowledgments

This work was partially supported by the Italian Minister of Education, University and Research through the PRIN project 2005020804.

References

- [1] S.Y. Chou, P.R. Krauss, P.J. Renstrom, *Science* 272 (1996) 85.
- [2] B. Heidari, I. Maximov, L. Montelius, *J. Vac. Sci. Technol.*, B 18 (2000) 3557.
- [3] D. Pisignano, A. Melcarne, D. Mangiullo, R. Cingolani, G. Gigli, *J. Vac. Sci. Technol.* B 22 (2004) 185.
- [4] J. Wang, X. Sun, L. Chen, S.Y. Chou, *Appl. Phys. Lett.* 75 (1999) 2767.
- [5] M. Yan, L.J. Rothberg, F. Papadimitrakopoulos, M.E. Galvin, T.M. Miller, *Phys. Rev. Lett.* 73 (1994) 744.
- [6] J.A. Rogers, Z. Bao, V.R. Raju, *Appl. Phys. Lett.* 72 (1998) 2716.
- [7] S. Noach, E.Z. Faraggi, G. Cohen, Y. Avny, R. Neumann, D. Davidov, A. Lewis, *Appl. Phys. Lett.* 69 (1996) 3650.
- [8] Y. Xia, G.M. Whitesides, *Angew. Chem. Int. Ed.* 37 (1998) 550.
- [9] J.A. Rogers, M. Meier, A. Dodabalapur, E.J. Laskowski, M.A. Cappuzzo, *Appl. Phys. Lett.* 74 (1999) 3257.
- [10] J.A. Rogers, Z. Bao, L. Dhar, *Appl. Phys. Lett.* 73 (1998) 294.
- [11] D.A. Pardo, G.E. Jabbour, N. Peyghambarian, *Adv. Mater.* 12 (2000) 1249.
- [12] H. Sirringhaus, T. Kawase, R.H. Friend, T. Shimoda, M. Inbasekaran, W. Wu, E.P. Woo, *Science* 290 (2000) 2123.
- [13] M. Colburn, S. Johnson, S. Damle, T. Bailey, B. Choi, M. Wedlake, T. Michaelson, S.V. Sreenivasan, J. Ekerdt, C.G. Willson, *Proc. SPIE* 3676 (1999) 379.
- [14] D. Pisignano, L. Persano, M.F. Raganato, P. Visconti, R. Cingolani, G. Barbarella, L. Favaretto, G. Gigli, *Adv. Mater.* 16 (2004) 525.
- [15] E. Mele, F. Di Benedetto, L. Persano, R. Cingolani, D. Pisignano, *Nano Lett.* 5 (2005) 1915.
- [16] D.-Y. Khang, H. Yoon, H.H. Lee, *Adv. Mater.* 13 (2001) 749.
- [17] R.H. Friend, R.W. Gymer, A.B. Holmes, J.H. Burroughes, R.N. Marks, C. Taliani, D.D.C. Bradley, D.A. Dos Santos, J.L. Brédas, M. Lögdlund, W.R. Salaneck, *Nature* 397 (1999) 121.
- [18] P.K.H. Ho, D.S. Thomas, R.H. Friend, N. Tessler, *Science* 285 (1999) 233.
- [19] F. Hide, M.A. Diaz-García, B.J. Schwartz, M.R. Andersson, Q. Pei, A.J. Heeger, *Science* 273 (1996) 1833.
- [20] N. Tessler, G.J. Denton, R.H. Friend, *Nature* 382 (1996) 695.
- [21] R. Xia, G. Heliotis, P.N. Stavrinou, D.D.C. Bradley, *Appl. Phys. Lett.* 87 (2005) 031104.
- [22] Q. Pei, G. Yu, C. Zhang, Y. Yang, A.J. Heeger, *Science* 269 (1995) 1086.
- [23] G. Yu, J. Gao, J.C. Hummelen, F. Wudl, A.J. Heeger, *Science* 270 (1995) 1789.
- [24] C.J. Brabec, N.S. Sariciftci, J.C. Hummelen, *Adv. Funct. Mater.* 11 (2001) 15.
- [25] V.L. Colvin, M.C. Schlamp, A.P. Alivisatos, *Nature* 370 (1994) 354.
- [26] X. Gong, S. Wang, D. Moses, G.C. Bazan, A.J. Heeger, *Adv. Mater.* 17 (2005) 2053.
- [27] M. Mazzeo, D. Pisignano, F. Della Sala, J. Thompson, R.I.R. Blyth, G. Gigli, R. Cingolani, G. Sotgiu, G. Barbarella, *Appl. Phys. Lett.* 82 (2003) 334.
- [28] J.M. Lupton, B.J. Matterson, I.D.W. Samuel, M.J. Jory, W.L. Barnes, *Appl. Phys. Lett.* 77 (2000) 3340.
- [29] http://p-o-weber.de/e_/presses/pw_e.html.
- [30] N.C. Greenham, I.D.W. Samuel, G.R. Hayes, R.T. Phyllips, Y.A.R.R. Kessener, S.C. Moratti, A.B. Holmes, R.H. Friend, *Chem. Phys. Lett.* 241 (1995) 89.
- [31] B.J. Matterson, J.M. Lupton, A.F. Safonov, M.G. Salt, W.L. Barnes, I.D.W. Samuel, *Adv. Mater.* 13 (2001) 123.
- [32] J.M. Ziebarth, A.K. Saafir, S. Fan, M.D. McGehee, *Adv. Funct. Mater.* 14 (2004) 451.